Effect of Si doping in wells of AlGaN/GaN superlattice on the characteristics of epitaxial layer*

Zhang Wei(张 伟)†, Xue Jun-Shuai(薛军帅), Zhou Xiao-Wei(周晓伟), Zhang Yue(张 月), Liu Zi-Yang(刘子阳), Zhang Jin-Cheng(张进成), and Hao Yue(郝 跃)

Key Laboratory of Wide Band-Gap Semiconductor Materials and Devices, Xidian University, Xi'an 710071, *China*

(Received 6 December 2011; revised manuscript received 9 January 2012)

An AlGaN/GaN superlattice grown on the top of a GaN buffer induces the broadening of the full width at half maximum of (102) and (002) X-ray diffraction rocking curves. With an increase in the Si-doped concentration in the GaN wells, the full width at half maximum of the (102) rocking curves decreases, while that of the (002) rocking curves increases. A significant increase of the full width at the half maximum of the (002) rocking curves when the doping concentration reaches 2.5×10^{19} cm^{-3} indicates the substantial increase of the inclined threading dislocation. High level doping in the AlGaN/GaN superlattice can greatly reduce the biaxial stress and optimize the surface roughness of the structures grown on the top of it.

Keywords: AlGaN/GaN, superlattice, Si doping

PACS: 71.55.Eq, 68.55.Ln, 68.65.Cd **DOI:** 10.1088/1674-1056/21/7/077103

1. Introduction

GaN and GaN-based materials have been widely used in anti-irradiation[1,2] and optoelectronic devices.[3,4] Interest in the AlGaN/GaN superlattice stems from the large band offset between the barrier and the well, with which the responsive wavelength of the intersubband photonic device can be tuned and cover telecommunication wavelengths.[5−7] Due to the large electron effective mass in GaN, the thickness of the well should not exceed 1.5 nm in order to satisfy the wavelength range from 1.3 μm to 1.55 μm. Further progress in this field requires much attention to the quality of epitaxial layers. Si doping plays an important role in determining the properties of superlattices.[8−10] It not only supplies electrons for the well, but also interacts with the internal polarization field, which modifies the positions of subbands greatly. Recently, our simulation results show that the high-level doping is a necessary condition for the realization of the AlGaN/GaN superlattice-based photodetector, otherwise the wells in the superlattice are depleted.[11] Moreover, the Si doping reduces the lifetime of carriers and the responsibility of photodetector. Based on the above facts, it is necessary to explore the influence of the Si doping on the characteristics of the superlattice structure.

In this paper, we demonstrate that the AlGaN/GaN superlattice, grown on the top of a 1.5-μm GaN buffer layer, induces an additional edge and screw threading dislocations (TDs) into the system. With an increase in the Si-doped concentration in the GaN wells, more edge TDs are bent in the superlattice. The inclined TDs act as screw TDs and broaden the full width at half maximum (FWHM) of the high-resolution X-ray diffraction (HRXRD) (002) rocking curve. The in-plane stress of the superlattice will decrease with the increase of the inclined TDs, and the surface roughness was simultaneously optimized.

2. Sample design and experimental setup

All the samples were grown with a self-designed cold-wall metal–organic chemical vapor deposition (MOCVD) system on the (0001) sapphire substrate. Firstly, an 8-nm high-temperature AlN nucleating layer was grown at 1020 °C. Secondly, a GaN buffer of 1.5 μm was grown directly on the top of the AlN. A

*Project supported by the National Key Science & Technology Special Project of China (Grant No. 2008ZX01002-002) and the Major Program and State Key Program of National Natural Science Foundation of China (Grant No. 60890191).

†Corresponding author. E-mail: zwxidian@mail.xidian.edu.cn

© 2012 Chinese Physical Society and IOP Publishing Ltd

Table 1. HRXRD, Raman and AFM data for the four different superlattice structures.

Structure	Doping in well/cm^{-3}	FWHM(002)/arcsec	FWHM(102)/arcsec	FWHM E_2/cm^{-1}	Surface roughness/nm
A	–	104.88	328.57	3.14	0.264
B	6.0×10^{16}	114.62	452.51	2.99	0.286
C	1.5×10^{18}	126.48	391.97	2.99	0.273
D	2.5×10^{19}	396.80	370.43	3.14	0.176

400-nm 1.5×10^{18} cm^{-3} Si-doped GaN was deposited before the growth of the superlattice. Except for sample A, a 20-period AlGaN/GaN (3 nm/3 nm) superlattice was then grown to be an active region and a 100-nm 1.5×10^{18} cm^{-3} Si-doped GaN was deposited as the cap layer. AlGaN barriers were nominally undoped. The Si-doped concentrations in the GaN wells for samples B, C, and D are 6.0×10^{16}, 1.5×10^{18}, and 2.5×10^{19} cm^{-3}, respectively. Sample A can be used as a reference. Table 1 shows some critical structural and experimental data obtained from HRXRD, Raman and atom force microscopy (AFM) measurements. As the doping concentration in the GaN wells increases, the FWHM of the (002) rocking curve increases, while that of the (102) rocking curve decreases. The variation of the FWHM of the E_2 Raman phonon frequency is negligible. Simultaneously, the surface roughness is improved greatly.

3. Results and discussion

3.1. High-resolution X-ray diffraction

The characteristics of superlattices have been assessed with HRXRD measurements. The ω–2θ scanning results of the (002) X-ray reflection for all wafers are shown in Fig. 1(a). The position of the satellite peaks of samples B, C, and D are almost identical, which means they have the same period thickness and Al fraction in the barriers.[12] These results ensure that the comparison made below only focuses on the difference of the Si-doped concentration in the GaN wells.

The values of FWHM for the (002) and (102) rocking curves are recorded in Table 1, and the spectra of the (002) rocking curves are presented in Fig. 1(b). Compared with sample A, samples B, C, and D have a broader FWHM on both of the rocking curves.[13] The TD density can be evaluated by this data. The specific TD geometry in a film will lead to distortions of only specific crystallographic planes.[14,15] Edge dislocations will only distort the (hkl) planes with nonzero h or k, while the $(00l)$ rocking curves are only sensitive to the screw TD content in the films. Assuming that the mixed dislocations are a mixture of the pure edge and pure screw TDs, then only the pure screw TDs influence the FWHM of the (002) rocking curve.

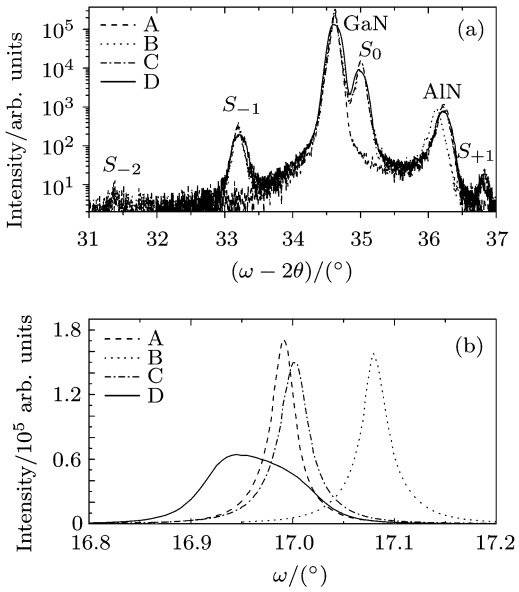


Fig. 1. (a) ω-2θ scanning results of the samples. The satellite peaks of the surperlattice are labeled as S_{+1}, S_0, S_{-1}, and S_{-2}. (b) Symmetric (002) rocking curves of the four samples.

The densities of the edge and the screw TDs increase from 2.2×10^7 and 5.7×10^8 to 2.6×10^8 cm^{-2} for sample A (without superlattice) and 1.1×10^9 cm^{-2} for sample B (with superlattice), respectively. The deposition of superlattice induces the increase in both of the edge and the screw TDs. With the increase of the Si-doped concentration in the wells of the superlattice, the edge TDs decrease while the screw TDs increase. As the doping concentration increases from 1.5×10^8 (sample C) to 2.5×10^9 cm^{-2} (sample D), the edge TDs decrease from 8.1×10^8 to 7.2×10^8 cm^{-2}, while the screw TDs increase significantly from 3.0×10^7 to 3.1×10^8 cm^{-2}.

3.2. Raman measurement

There are three possible reasons for the increase of the screw TDs. Firstly, the influence of the superlattice on the crystalline quality of the underlying

GaN buffer. Secondly, another 3D to 2D nucleation process as at the substrate/buffer interface. Thirdly, the increase of the inclined TDs which has an influence on the FWHM of the (002) rocking curves. The drastic change of the screw TDs first spurs us to wonder whether the existence of superlattices has an influence on the crystalline quality of the underlying buffer layer in the cooling process, because the screw TDs are not likely to form elsewhere but at the substrate/buffer interface.[16,17] Raman measurement was performed to resolve our doubt. The measurements were conducted in backscattering $Z(xx)\overline{Z}$ geometry. The spectrum obtained with a 514-nm excitation reflects the average GaN crystalline quality. As seen from Table 1, the slender difference between the FWHM of the E_2 modes, which reflects the crystalline quality of the bulk GaN, indicates that the buffer layers are unaffected by the growth of superlattices, and the additional TDs shown in the rocking curves are limited in or on the top of the superlattice. The latter AFM results do not support a new 3D growth model at the buffer/superlattice interface either. Thus, it is more likely that the broadening of the (002) rocking curve is attributed to the formation of inclined TDs.[18]

Superlattices grown at the substrate/buffer interface can reduce the density of punch-through TDs by a recombination and annihilation process.[19–21] There is a high density of TDs in AlGaN barriers. Some of them extend to the surface and others interact with the edge TDs originated from the buffer. The interaction can induce the formation of an inclined TD with line direction different from that of the edge TDs ($\langle 0001 \rangle$). The inclined TDs contribute to the broadening of the (002) XRD rocking curve because of the variation of the stress situation in the (002) plane. For some reason, perhaps the variation of the atom mobility, the Si doping can increase the opportunity of the formation of the inclined TDs, especially when the doping concentration reaches the order of 10^{19} cm^{-3}.

Raman spectra under a 325-nm excitation are presented in Fig. 2(b). These spectra reflect crystalline qualities of the 40-nm GaN under the surface. Comparison between 514-nm and 325-nm excitation spectra provides us with information about the evolvement of the stress situation after the development of the superlattice. From the 514-nm excited Raman spectrum, we can see that all the buffer layers are under compressive stress, because the values of the E_2 peak are larger than those of the unstrained GaN (567 cm^{-1}). Only A_1(LO) photons can be seen in Fig. 3(b), due to the strong background photoluminescence signal. Although commonly used to evaluate the doped concentration, the A_1(LO) phonon can also be used to extract the stress situation in materials.[22,23] The variation of the A_1(LO) phonon manifests the same trend as that of the E_2, which can be seen clearly in Fig. 2(a).

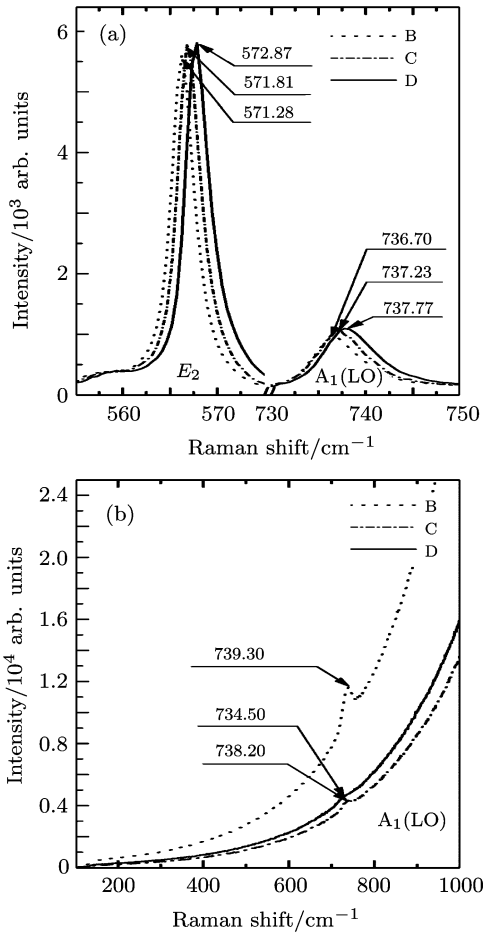


Fig. 2. Raman results under (a) 514-nm and (b) 325-nm excitations.

For GaN, the phonon frequency of A_1(LO) shifts linearly with biaxial stress at a rate of 0.8 cm^{-1}GPa^{-1} for biaxial stress. The A_1(LO) peak variation between the 514-nm and 325-nm excitations for samples B, C, and D are –2.60, –0.97, and 3.27 cm^{-1}, respectively. The negative values indicate the increase of the compressive stress, while the positive values demonstrate its decrease. Compared with that in the GaN buffer, the compressive stress in the GaN cap layer of sample D decreases by 2.6 GPa^{-1} and reaches the quasi-unstrained state (734 cm^{-1} for unstrained GaN). The decrease of the compressive stress in the GaN cap layer is attributed to the formation of the inclined TDs which are induced by high-concentration Si doping in the GaN well.

3.3. Atom force microscopy

The surface morphology was analyzed through AFM measurements, as shown in Fig. 3. Terraces separated by a high step of 2–3 Å are clearly visible. The parallel and straight terraces suggest the existence of the step flow growth mode, which means the two-dimensional layer growth. Roughness measured in a 5 μm × 5 μm area for samples B, C, and D are 0.286, 0.273, and 0.176 nm, respectively. Compared with sample B, the surface roughness of sample D decreases by 35%. The surface roughness decreases from 0.273 to 0.176 nm as the doping concentration in wells increases from 1.5×10^8 to 2.5×10^9 cm^{-2}. The surface roughness was converted from the variation of the voltage at the ends of piezo cantalever. For samples B, C, and D, the number of pits deeper than 1 nm are 1.52×10^8, 1.48×10^8, and 5.2×10^7 cm^{-2}, respectively. The density of pits obviously decreases for sample D, which indicates the reduction of punch-through TDs.

From the discussion about XRD and Raman measurements, we have predicted that the interaction between edge TDs can induce the formation of inclined TDs with a line direction different from that of the edge TDs (⟨0001⟩). The formation of those inclined TDs reduces the number of the TDs which have the opportunity to penetrate through the superlattice and leaves relevant pits on the surface. The results from the AFM measurements verity this prediction. Thus, it is reasonable for us to predict that a majority of the inclined TDs with line direction are parallel to the AlN/GaN interface and do not intersect with the surface. This result is consistent with the formation process of interface misfit dislocation. As reported by Bai *et al.* in Ref. [24], most of the TDs do not propagate into the upper structure of the AlN nucleating layer, but interact with each other.

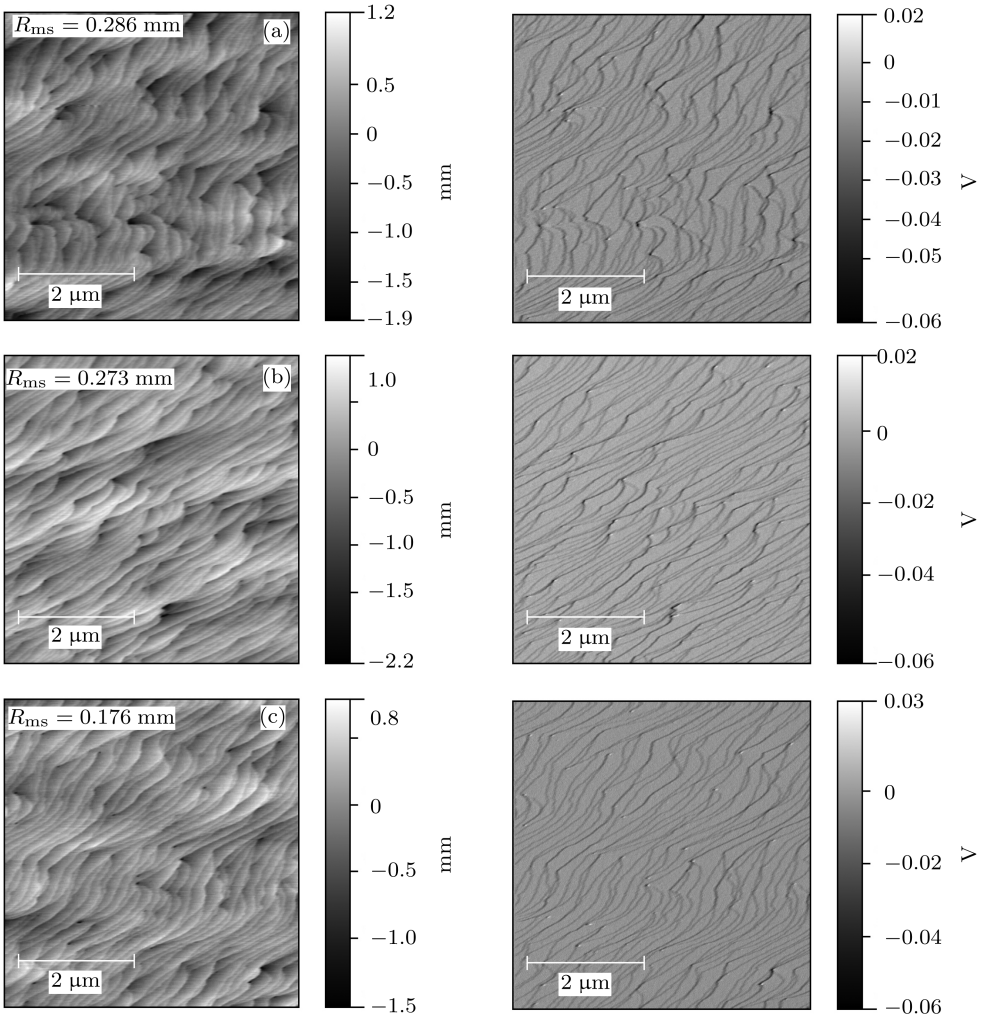


Fig. 3. The AFM images of samples (a) B, (b) C, and (c) D. In order to observe the parallel and straight terraces, fluctuation of the corresponding voltage is presented on the right for samples (d) B, (e) C, and (f) D.

4. Conclusions

In conclusion, an AlGaN/GaN superlattice grown on the top of the GaN buffer introduces additional TDs in the structure. Comparison between the XRD and Raman results indicates that the TDs do not originate from the buffer layer. With the increase of doping in the wells of the superlattice, more edge TDs are bent. The inclined TDs increase the FWHM of the XRD (002) rocking curve and act as screw TDs. A majority of the inclined TDs with line direction are parallel to the surface and do not disrupt the surface roughness. The stress situation in the AlGaN/GaN superlattice can also be greatly influenced by the doping. The surface roughness has been optimized by the appearance of the inclined TDs and the relaxation of the stress. The obtained results are helpful to analyze the optical and electrical properties of superlattice-based devices, and also can be used to optimize the quality of GaN epitaxial layer grown on heterogenous substrates.

References

[1] Khanna R, Allums K K, Abernathy C R, Pearton S J, Kim J, Ren F, Dwivedi R, Fogarty T N and Wilkins R 2004 *Appl. Phys. Lett.* **85** 3131

[2] Luo B, Johnson J W, Ren F, Allums K K, Abernathy C R, Pearton S J, Dwivedi R, Fogarty T N, Wilkins R, Dabiran A M, Wowchack A M, Polley C J, Chow P P and Baca A G 2001 *Appl. Phys. Lett.* **79** 2196

[3] Zhu T G, Chowdhury U, Denyszyn J C, Wong M M and Dupuis R D 2003 *J. Cryst. Growth* **248** 548

[4] Dadgar A, Hums C, Diez A, Blasing J and Krost A 2006 *J. Cryst. Growth* **297** 279

[5] Heber J D, Gmachl C, Ng H M and Cho A Y 2002 *Appl. Phys. Lett.* **81** 1237

[6] Gmachl C, Ng H M, Chu S N G and Cho A Y 2000 *Appl. Phys. Lett.* **77** 3722

[7] Hofstetter D, Baumann E, Giorgetta F R, Graf M, Maier M, Guillot F, Bellet-Amalric E and Monrot E 2006 *Appl. Phys. Lett.* **88** 121112

[8] Kandaswamy P K, Machhadani H, Kostar Y, Sakr S, Das A, Tchernycheva M, Rapenne L, Sarigiannidou E, Julien F H and Monroy E 2010 *Appl. Phys. Lett.* **96** 141903

[9] Machhadani H, Kandaswamy P, Sakr S, Vardi A, Wirtmuller A, Nevou L, Guillot F, Pozzovivo G, Tchernycheva M, Lupu A, Vivien L, Crozat P, Warde E, Bougerol C, Schacham S, Strasser G, Bahir G, Monroy E and Julien F H 2009 *New J. Phys.* **11** 125023

[10] Kandaswamy P K, Guillot F, Bellet-Amalric E, Monroy E, Nevou L, Tchernycheva M, Michon A, Julien F H, Baumann E, Giorgetta F R, Hofstetter D, Remmele T, Albrecht M, Birner S and Dang L S 2008 *J. Appl. Phys.* **104** 093501

[11] Zhang W, Zhang Y, Xue J S, Zhang Y, Lü L, Zhang J C and Hao Y 2011 *Appl. Phys. Lett.* **99** 162105

[12] Moram M A and Vickers M E 2009 *Rep. Prog. Phys.* **72** 036502

[13] Metzger T, Hopler R, Born E, Ambacher O, Stutzmann M, Stommer R, Schuster M, GoBel H, Christiansen S, Albrecht M and Strunk H P 1998 *Philos. Mag.* A **77** 1013

[14] Heying B, Wu X H, Keller S, Li Y, Kapolnek D, Keller B P, DenBaars S P and Speck J S 1996 *Appl. Phys. Lett.* **68** 643

[15] Heinke H, Kirchner V, Einfeldt S and Hommel D 2000 *Appl. Phys. Lett.* **77** 2145

[16] Mathis S K, Romanov A E, Chen L F, Beltz G E, Pompe W and Speck J S 2001 *J. Crysta. Growth* **231** 371

[17] Germain M, Leys M, Boeykens S, Degroote S, Wang W F, Schreurs D, Ruythooren W, Choi K H, Daele B V, Tendeloo G V and Borghs G 2003 *Mat. Res. Soc. Symp. Proc.* **798** Y10.22

[18] Weng X, Acord J D, Jain A, Dickey E C and Redwing J M 2007 *J. Electron. Mater.* **36** 346

[19] Feltin E, Beaumont B, Laugt M, Mierry P D, Vennegues P, Lahreche H, Leroux M and Gibart P 2001 *Appl. Phys. Lett.* **79** 3230

[20] Nikishin S A, Faleev N N, Antipov V G, Francoeur S, de Peralta L G, Seryogin G A, Temkin H, Prokofyeva T I, Holtz M and Chu S N G 1999 *Appl. Phys. Lett.* **75** 2073

[21] Liaw H M, Venugopal R, Wan J and Melloch M R 2001 *Solid-State Electron.* **45** 1173

[22] Kuball M 2001 *Surf. Interface. Anal.* **31** 987

[23] Demangeot F, Frandon J, Renucci M A, Briot O, Gil B and Aulombard R L 1996 *Solid State Commun.* **100** 207

[24] Bai J, Wang T, Lee K B, Parbrook P J, Wang Q and Cullis A G 2001 *Surf. Interface. Anal.* **602** 2643